Controlling the Propagation of X-Ray Waves inside a Heteroepitaxial Crystal Containing Quantum Dots Using Berry's Phase

Yoshiki Kohmura,[1] Kei Sawada,[1] Susumu Fukatsu,[2] and Tetsuya Ishikawa[1]

[1]RIKEN SPring-8 Center, 1-1-1, Kouto, Sayo-gun, Sayo-cho, Hyogo 679-5148, Japan

[2]The University of Tokyo, Graduate School of Arts and Sciences, Komaba, Tokyo 153-8902, Japan

(Received 26 October 2012; published 28 January 2013)

We study a new aspect of the Berry-phase effect as the collaborative x-ray translation by a crystal with undulated deformation. The macroscopic translation was observed around the interface of a heteroepitaxial crystal deformed by quantum dots of 4.1 germanium monolayers on a silicon substrate. The quantum dots formed a large local gradient of deformation at the interface, which triggered the x-ray translation into two directions. This effect provides a new probe for investigating the interfacial strain, and leads to a single-crystal beam splitter with parallel exit beams.

DOI: 10.1103/PhysRevLett.110.057402 PACS numbers: 78.70.Ck, 41.50.+h, 83.85.Hf

The extensive growth of nanotechnology enables us to manipulate the optical fields by materials fabricated at the nanoscale. For example, the development of waveguides and lasers is accelerated by controlling visible light with photonic crystals. Following this trend, we intend to control the x-ray trajectories by designing materials at the atomic scale. However, the extremely small interaction between x rays and matter has been an obstacle for the development of x-ray optics. One hint to solve such a difficulty is the huge x-ray translation effect in deformed crystals, predicted by the Berry-phase theory [1]. This effect was experimentally verified as translation over a millimeter distance in a deformed silicon crystal [2]. However, the theory and the experiment concerned crystals with a simple monotonic bend. We should move on to investigate crystals with flexible strain fields, in search of a more practical material for designing optics. As a demonstration, we used a heteroepitaxial silicon crystal having germanium quantum dots (QDs) on its interface. The QDs strain the crystal and produce lattice deformation according to their spatial distribution. Under such strain, an x-ray translation effect is naively expected to be cancelled or averaged. Beyond such an assumption, we discovered a new x-ray phenomenon, a macroscopic x-ray translation due to the collaborative effects. We found that QDs offer not only rich electronic properties depending on their size and density but also an interesting setting for developing x-ray optics.

We will first discuss the theoretical background of x-ray propagation through a crystal with strain. Most research on x-ray diffraction inside deformed crystals relies on the well known theories, such as the Takagi-Taupin theory [3–5] and the eikonal theory [6]. These theories are suited for detailed simulations, but the effect of strain on x-ray propagation cannot be derived in a straightforward way. Here we focus on another theory, related to the Berry phase. This theory gives a more intuitive picture of how the strain field affects x-ray propagation. In a perfect crystal, x-ray wave packet propagation is determined by the dispersion relation and is described by the group velocity $\vec{v}_g = \nabla_k \omega(\vec{k})$, where $\vec{k}$ is the wave vector, as shown in Fig. 1(a). Because of the gap Δk around the Bragg condition, $|\vec{k}| \simeq |\vec{k} + \vec{G}|$, the group velocity is very sensitive to the incident angle, θ. In the presence of the strain field, the propagating direction differs from the group velocity. Wave packet propagation in a deformed crystal is described by the equation of motion for its center position $\vec{r}$ to be

$$\frac{dr_a}{dt} = (\vec{v}_g)_a + \sum_b \frac{dr_b}{dt} \Omega_{k_a r_b} \qquad (a, b = x, y, z), \qquad (1)$$

where $\Omega_{k_a r_b}$ is the Berry curvature tensor, represented as a product of functions in the reciprocal space and in the real space,

$$\Omega_{k_a r_b} = f_{k_a}(\vec{k}) g_{r_b}(\vec{r}). \qquad (2)$$

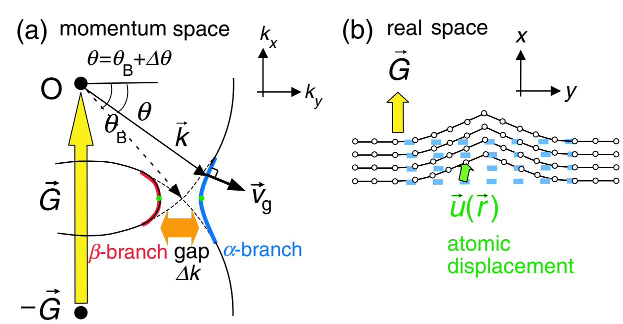

FIG. 1 (color online). Schematic diagrams of the fundamental settings. (a) Dispersion relation in two-dimensional momentum space for x-ray propagation inside crystals. A cross-sectional view on the fixed angular frequency, ω, is shown. The α branch and β branch correspond to the curves with the incidence angle slightly lower and higher than the Bragg angle. (b) The atomic displacement, from $\vec{r}$ to $\vec{r} + \vec{u}(\vec{r})$, in real space for the undulated crystal planes around the interface of heteroepitaxial crystals.

Here

$$f_{k_a}(\vec{k}) = \pm \frac{(e_{\vec{k}+\vec{G}})_a - (e_{\vec{k}})_a}{2[(\Delta k)^2 + \frac{1}{4}(|\vec{k}| - |\vec{k}+\vec{G}|)^2]^{3/2}}(\Delta k)^2 \quad (3)$$

represents a profile in momentum space. Its double sign, $\pm$, corresponds to the α and β branches [Fig. 1(a)], respectively, and $e_{\vec{k}} = \vec{k}/|\vec{k}|$. A profile in real space is represented by the local gradient of deformation to be

$$g_{r_b}(\vec{r}) = \frac{\partial[\vec{G}\cdot \vec{u}(\vec{r})]}{\partial r_b}, \quad (4)$$

where $\vec{u}(\vec{r})$ represents the atomic displacement vector as shown in Fig. 1(b). The first term on the right-hand side of Eq. (1) is the group velocity that represents the usual propagation of x rays in a perfect crystal. The second term, related to the Berry curvature in phase space, is the effect of the atomic displacement coupled to the x-ray dynamical diffraction. The value of this term becomes maximum at the Bragg condition, $|\vec{k}| = |\vec{k}+\vec{G}|$. We will focus on this second term and experimentally demonstrate its unusual effects.

The interface of a heteroepitaxial crystal often contains strain with the angular undulation of deformation larger than the intrinsic Darwin width of the substrate crystal, W. In such cases, the theory assuming only a single reciprocal vector, $\vec{G}$, is no longer valid [1]. However, the validity of the theory is recovered if we define two reciprocal lattice vectors, $\vec{G}_1$ and $\vec{G}_2$, at characteristic positions on the slopes. We define two pairs of points where the reciprocal lattice vectors are tilted from the top or the bottom of the crystal plane (CP) by the angle γW in the anticlockwise and the clockwise directions. The incident angles of x rays onto the CP are $\theta_B + \gamma W$ at points P_1 and P_3 and $\theta_B - \gamma W$ at points P_2 and P_4 as shown in Fig. 2(a). The schematic Bragg reflected intensity profiles are shown for the cases of $\gamma < 1/2$ and $1/2 < \gamma < 1$ in Figs. 2(b) and 2(c). Clearly, only one reciprocal vector is needed for the former, while two reciprocal vectors are needed for the latter. Hereafter we deal with the case of $1/2 < \gamma < 1$, where a simultaneous excitation of the two branches is observed as in Fig. 2(c). As shown in Eq. (2), the x-ray translation effect due to the local CP is affected by the sign of the local gradient of deformation along the y axis, $g_y(\vec{r})$, which is inverted by switching the side, the left or the right side, of P_1–P_4 as shown in Figs. 2(d) and 2(e). This effect is also affected by the branch on the dispersion curve as summarized in Table I. Note that the vector of Eq. (3) around the Bragg condition is approximately parallel to the reciprocal vector, which causes the translation to occur mainly along the x axis in Figs. 1(b), 2(a), 2(d), and 2(e).

For the experiment, we prepared a silicon heteroepitaxial crystal strained by Ge QDs grown at the interface. Because of the larger lattice constant of germanium compared with that of silicon, a tensile tension on the silicon

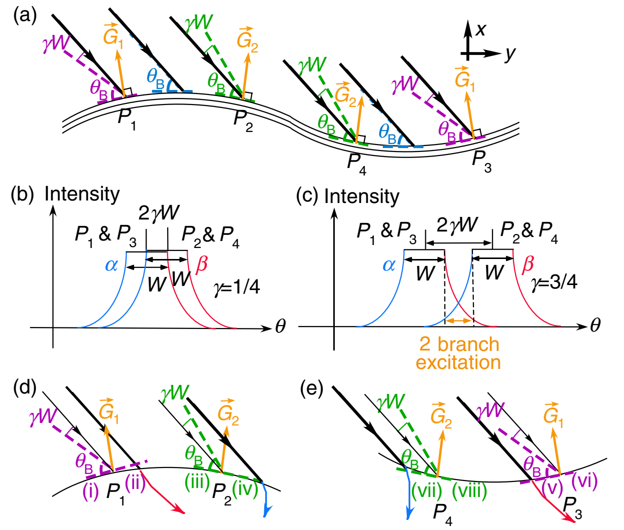

FIG. 2 (color online). (a) Two pairs of points P_1 and P_2, and P_3 and P_4 are defined to model the x-ray translation effect on the undulated crystal plane. The reciprocal lattice vectors at these points are represented as $\vec{G}_1$ and $\vec{G}_2$. (b) and (c) Schematic reflected intensity profile as a function of the incident angle at P_1–P_4 assuming $\gamma = 1/4$ (b) and $\gamma = 3/4$ (c). The α and β branches are simultaneously excited in the case of (c). Magnified views of the convex and concave regions of (a) are shown in (d) and (e), respectively, showing how the x-ray energy flows associated with the α and β branches are deviated. For the case of $1/2 < \gamma < 1$, the x-ray translation due to the local CP depends on the sign of local gradient of deformation along the y axis, $g_y(\vec{r})$ in Eq. (4). Expected trajectories crossing the four regions of the CP are exemplified.

substrate is induced beneath the Ge QDs. This effect causes the undulation of the substrate CP beneath the interface. The schematic diagram of such local lattice distortions is reported for the case of SiGe layers on a Si substrate [7]. We used the sample having Ge QDs [8] with a typical separation shorter than 1 μm on a 100 μmt silicon crystal. The Ge layer thickness was 4.1 monolayers where the Ge quantum dots start to be formed on the silicon substrate [9].

TABLE I. Dependence of the x-ray translation effect on the branch and on the local gradient of deformation at the regions (i)–(viii) in Figs. 2(d) and 2(e). See Eqs. (1)–(4) for the definitions of the variables and the tensor.

Region	Branch	$\mathrm{sgn}[f_{k_x}(\vec{k})]$	$\mathrm{sgn}[g_y(\vec{r})]$	$\mathrm{sgn}[\Omega_{k_x y}]$
(i)	β	−	+	−
(ii)	β	−	−	+
(iii)	α	+	+	+
(iv)	α	+	−	−
(v)	β	−	−	+
(vi)	β	−	+	−
(vii)	α	+	−	−
(viii)	α	+	+	+

We performed an experiment using a 15 keV x-ray beam at the undulator beam line BL29XU of SPring-8 [10]. We set the x-ray incidence angle onto the sample crystal close to the Bragg angle, $\theta_B = 17.6$ degrees for the silicon (400) plane as shown in Fig. 3(a) [11]. The transmitted x-ray images through the crystal were taken with an x-ray imaging detector [11] at various incidence angles in order to clarify the nature of the x-ray translation by the interfacial strain of the heteroepitaxial crystal.

Figure 3(b) shows the vertical intensity profiles as a function of the position at the detector, y_d. When the offset angle from the Bragg angle $\Delta\theta$ is larger than the intrinsic Darwin width, e.g., $\Delta\theta = +5.5'' > W \simeq 2''$, a single peak was observed at the detector position $y_d \simeq 0$ μm as shown in Fig. 3(b), coinciding with the incident beam position. The observed intensity profiles showed a dramatic change in the range of $-4'' \leq \Delta\theta \leq +5.5''$, where the peak position is shifted or translated into the region $y_d < 0$ μm and the region $y_d > 0$ μm. The observed amount of translation is plotted as a function of $\Delta\theta$ in Fig. 3(c). This shows that the angular dependences of the peak position in these two regions are completely different. We put the offset angles to be $\Delta\theta_1 = 0''$ and $\Delta\theta_2 = -2''$, where the amount of translation is maximum in the negative and in the positive direction. The translation of the peak, from the incident beam position into $y_d < 0$ μm and into $y_d > 0$ μm, is enlarged for $\Delta\theta$, approaching $\Delta\theta_1$ from the negative side and approaching $\Delta\theta_2$ from the positive side as shown by solid lines in Fig. 3(c). These correspond to x-ray translations on the α and β branches [Fig. 1(a)] at which x rays travelled towards the independent directions. Figure 3(c) also justifies the theoretical calculation, shown with dotted lines, by the remarkable match with the experimental data.

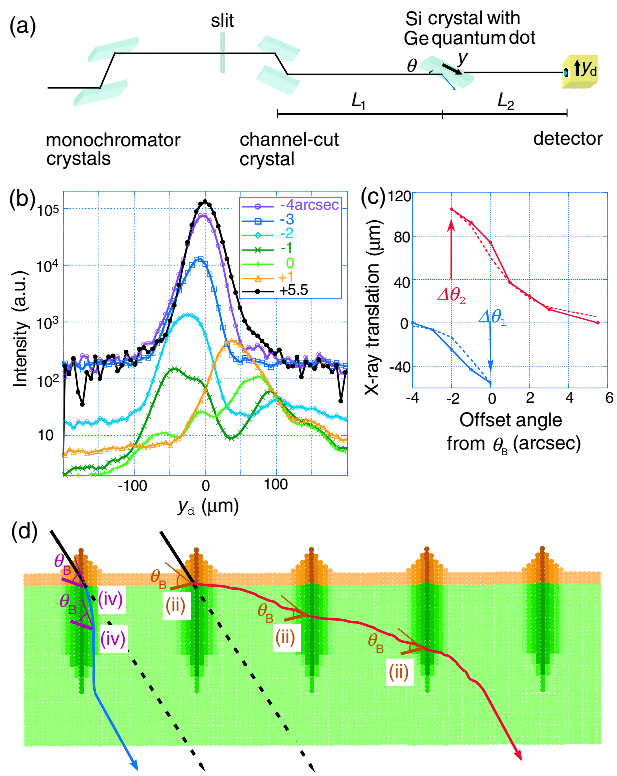

FIG. 3 (color online). Experimental setup, result, and model. (a) Schematic diagram of the experimental setup. For details, see Ref. [11]. (b) Measured intensity profiles along the vertical axis on the x-ray imaging detector for seven offset angles. (c) Measured translation from the incident beam position, $y_d = 0$ μm, as a function of the offset angle from the Bragg angle, $\Delta\theta$. Solid lines show the negative and positive translation on the α and β branches, while dotted lines represents the theoretical results. (d) Model of the collaborative translation. Germanium and silicon atoms are schematically represented by circles with different colors with the graduation showing the amount of deformation. The x rays undergo repeated local translation when they pass through region (ii) with $\Delta\theta > 0$ and region (iv) with $\Delta\theta < 0$ as in Fig. 2(d).

Simultaneous translation into two directions on the two different branches is clearly observed in Fig. 3(c), at $\theta_B + \Delta\theta_2 \leq \theta \leq \theta_B + \Delta\theta_1$, which supports our model in Fig. 2(c). The angular difference of the two slopes of the CPs is $(\Delta\theta_1 - \Delta\theta_2) + W \simeq 4''$ and is larger than the intrinsic Darwin width of the perfect crystal, $W \simeq 2''$ for the given condition. The present method offered the capability of detecting a weak interfacial strain at a length scale shorter than 1 μm.

Because of a glazing incidence effect, the measured amount of translation at the detector plane is 3.3 times larger at the surface of the crystal. Therefore, the x-ray translations at the detector plane, up to $+105$ μm on the β branch and up to -56 μm on the α branch [Fig. 3(c)], correspond to $+347$ μm [12] and -185 μm at the surface of the silicon crystal, respectively. Table I shows that the translations in the positive and the negative directions on the observed branch are due to the x rays passing through regions (ii) and (iv) on the convex CP or (v) and (vii) on the concave CP as shown in Figs. 2(d) and 2(e). On the other hand, the Ge QDs exert tensile strain onto the silicon substrate, because of the mismatch of the lattice constant. This causes the CPs beneath the QDs to be deformed into a convex shape towards the surface as shown in Fig. 2(d) with a large local gradient of deformation as modeled in Fig. 3(d). To conclude, the observed translation into two directions should have occurred by x rays passing through regions (ii) and (iv). Note that the changes of the wave vector of the x rays are negligible through the propagation inside the crystal. This causes the exit beam in two directions to propagate parallel to the incident beam.

The dramatic angular dependence was preserved even if the irradiated positions on the sample are shifted or the crystal is rotated in plane. This suggests that the observed phenomenon is caused by the local strain of individual Ge QDs rather than by a single or a few anomalous QDs. It is interesting that the averaging effect by the huge number of Ge QDs in the x-ray beam is not significant. The observed amounts of the x-ray translation, $+347\ \mu$m and $-185\ \mu$m, are much larger than the typical interval of the QDs shorter than 1 μm [9]. These results support the model in Fig. 3(d) where a repeated and collaborative x-ray translation occurs through hundreds of layers of undulated CPs beneath the interface. The sharp angular dependence of the x-ray translation is efficient in revealing the buried local strain underneath the interfaces, which is inaccessible with other existing experimental techniques. Namely, in-depth strain information is limited with transmission electron microscopy [13] and atomic force microscopy [14]. Other methods, such as x-ray scattering methods [15], photoluminescence methods [8], and polarized Raman spectroscopy [16], are insensitive to the local strain because of the averaging effect over the illuminated area.

To summarize, we observed the collaborative Berry-phase effect of an x-ray translation beneath the interface of a silicon substrate having 4.1 germanium monolayers with quantum dots. The translations, by amount of 0.2 and 0.3 mm, were observed in two independent directions on the two branches of the dispersion surface. The regions with a large local gradient of deformation are clearly detected. This provides opportunities for the study of the strain field at the interface of heteroepitaxial crystals. Our result shows that a beam splitter with parallel exit beams, realized by the x-ray translation effect from a single crystal, will be a unique tool for x-ray pump-probe experiments and x-ray interferometry.

The authors express gratitude to M. Takahashi for fruitful discussions. This research was supported by KAKENHI (21340086, 22109005) from JSPS of Japan.

[1] K. Sawada, S. Murakami, and N. Nagaosa, Phys. Rev. Lett. **96**, 154802 (2006).

[2] Y. Kohmura, K. Sawada, and T. Ishikawa, Phys. Rev. Lett. **104**, 244801 (2010).

[3] S. Takagi, Acta Crystallogr. **15**, 1311 (1962).

[4] S. Takagi, J. Phys. Soc. Jpn. **26**, 1239 (1969).

[5] D. Taupin, Bull. Soc. Fr. Mineral. **87**, 469 (1964).

[6] A. Authier, *Dynamical Theory of X-ray Diffraction* (Clarendon, Oxford, 2001).

[7] K. Brunner, Rep. Prog. Phys. **65**, 27 (2002).

[8] H. Sunamura, N. Usami, Y. Shiraki, and S. Fukatsu, Appl. Phys. Lett. **66**, 3024 (1995).

[9] The sample Ge quantum dots were grown by vapor phase epitaxy on a Si(001) substrate at 700 degrees C. Si_2H_6 and GeH_4 were used as the source gases for Si and Ge, respectively. The separation of Ge QDs was measured by atomic force microscopy. The silicon crystal was thinned from the blank side into 100 μmt by a mechanochemical polishing method to reduce the absorption. The size of the crystal was 15 mm square.

[10] K. Tamasaku, Y. Tanaka, M. Yabashi, H. Yamazaki, N. Kawamura, M. Suzuki, and T. Ishikawa, Nucl. Instrum. Methods Phys. Res., Sect. A **467–468**, 686 (2001).

[11] At the upstream of the sample crystal, a vertical confining slit was placed to reduce the illuminated area on the sample crystal. A channel-cut crystal was set upstream of the sample to realize a narrow energy band width and a narrow angular divergence. At the downstream of the sample crystal, a phosphor coupled x-ray camera was placed to record the transmitted x-ray image. The distances were $L_1 = 1.1$ m and $L_2 = 0.5$ m in Fig. 3(a).

[12] The largest measured translation was 347 μm. The same amount of translation is obtained by a deformation of approximately 5 nm inside a deformed silicon crystal with a monotonic bend [1,2].

[13] R. Apetz, L. Vescan, A. Hartmann, C. Dieker, and H. Luth, Appl. Phys. Lett. **66**, 445 (1995).

[14] P. Schittenhelm, M. Gail, and G. Abstreiter, J. Cryst. Growth **157**, 260 (1995).

[15] Z. M. Jiang, X. M. Jiang, W. R. Jiang, Q. J. Jia, W. L. Zheng, and D. C. Qian, Appl. Phys. Lett. **76**, 3397 (2000).

[16] X. Wang, Z.-m. Jiang, H.-j. Zhu, F. Lu, D. Huang, X. Liu, C.-w. Hu, Y. Chen, Z. Zhu, and T. Yao, Appl. Phys. Lett. **71**, 3543 (1997).